

Simulation of 1D arterial flow in compliant bifurcating vessels.

Chayut Teeraratkul ^{*1}

¹Department of mechanical engineering, University of Colorado Boulder

Abstract

Three dimensional simulations of arterial blood flow provide detailed description of arterial flow features. Simulation 3D blood flow in a full arterial network is prohibitively expensive. In this work, a finite element based simulation of the 1D arterial flow model is presented. The model is obtained from averaging the Navier-Stokes equation over a cross-sectional area of in the cylindrical domain. An algebraic relation based on a generalized string model is used to couple pressure and the vessel's cross-sectional area. A domain decomposition approach based on the system's characteristics is used to account for bifurcations and possible discontinuities in vessel wall properties. The method is implemented using an open source finite element package FEniCS [1], and the code is available at <https://github.com/cteerara/Artery1D>

Keywords: blood flow models; finite elements; cardiovascular system

1 Introduction

Quantification of wave propagation phenomena in human circulation system is important to understanding and assessing human cardiovascular health. Three dimensional simulations can provide detailed description of local flow features, but these simulations are expensive to conduct. Human circulatory system consist of a complex network of compliant blood vessels from the arteries to arterioles to capillaries. A fully resolved 3D simulations of flow features in the arterial network are prohibitively expensive. One dimensional models for arterial blood flow can be devised and used to quantify the wave propagation phenomena in an arterial network at a relatively smaller computational cost. These one dimensional model can also be used assess wave propagation phenomena in the presence of arterial prosthesis [5] or used to inform downstream phenomena for a three dimensional simulation [4].

2 Methodology

2.1 One dimensional blood flow in compliant vessel

The models derivation is shown in [3] and will not be reproduced in this report. Here will will present the main underlying assumptions and the final system of the model.

^{*}chayut.teeraratkul@colorado.edu

The one dimensional blood flow model is derived from the incompressible Navier-Stokes equation in a cylindrical domain

$$\frac{\partial \mathbf{u}}{\partial t} + \mathbf{u} \cdot \nabla \mathbf{u} = \frac{1}{\rho} \nabla P + \nu \nabla^2 \mathbf{u}, \quad \nabla \cdot \mathbf{u} = 0 \quad (1)$$

with the assumptions that flow is axially symmetric. The model further assumes that flow in the axial direction is dominant, i.e., $u_r = u_\theta = 0$. The axial flow u_z is assumed to be constant over the cross section and equal to averaged flow \bar{u} over the cross section. Vessel wall displacement is also assumed to be axially symmetric and only displaced in the radial direction. By using the above assumptions, one will arrive at the following system of PDE

$$\begin{aligned} \frac{\partial A}{\partial t} + \frac{\partial Q}{\partial z} &= 0 \\ \frac{\partial Q}{\partial t} + \frac{\partial}{\partial z} \left(\alpha \frac{Q^2}{A} \right) + \frac{A}{\rho} \frac{\partial P}{\partial z} + K_R \frac{Q}{A} &= 0 \end{aligned} \quad (2)$$

where Q is the volume flow rate and P is the arterial pressure, and A is the cross-sectional area of the vessel. α is the momentum correction coefficient defined as

$$\alpha = \frac{\int u_z^2 dA}{A \bar{u}^2} \quad (3)$$

The parameter α depends the assumed radial profile of u_z . For parabolic profile, $\alpha = \frac{4}{3}$. K_R is related to the viscous effect of the flow. For a parabolic profile, $K_R = 8\pi\nu$.

To complete this model, a constitutive relation linking wall displacement and arterial pressure is needed. For this implementation, we assume that the vessel wall deformation is dominated by the elastic response which is the case for small vessel deformation. Using this assumption, we get a simple algebraic relation for pressure and cross-sectional area as follows

$$\begin{aligned} P - P_{ext} &= \beta \frac{\sqrt{A} - \sqrt{A_0}}{\sqrt{A_0}} \\ \beta &= E h_0 \sqrt{\pi} \end{aligned} \quad (4)$$

where E is the vessel wall's elastic modulus, and h_0 is wall thickness. A_0 is the initial vessel cross-sectional area and without loss of generality, we often assume that the external pressure $P_{ext} = 0$.

In this work, we further assumes that the initial cross-sectional area and wall properties are constant over the whole cylindrical section. A method to simulate variable wall properties will be described in the next section.

2.2 Characteristics analysis

After some manipulations, equations 2 with constant A_0 and β can be written in conservative form as

$$\frac{\partial \mathbf{U}}{\partial t} + \frac{\partial \mathbf{F}}{\partial z}(\mathbf{U}) = \mathbf{B}(\mathbf{U}) \quad (5)$$

where

$$\begin{aligned} \mathbf{U} &= \begin{bmatrix} A \\ Q \end{bmatrix} \\ \mathbf{F} &= \begin{bmatrix} Q \\ \alpha \frac{Q^2}{A} + \frac{\beta}{3\rho A_0} A^{3/2} \end{bmatrix} \\ \mathbf{B} &= \begin{bmatrix} 0 \\ K_R \frac{Q}{A} \end{bmatrix} \end{aligned} \quad (6)$$

The flux Jacobian of this hyperbolic system is

$$\mathbf{H} = \frac{\partial \mathbf{F}}{\partial \mathbf{U}} = \begin{bmatrix} 0 & 1 \\ -\alpha \frac{Q^2}{A^2} + \frac{\beta}{2\rho A_0} A^{1/2} & 2\alpha \frac{Q}{A} \end{bmatrix} \quad (7)$$

It is shown in [3] that for $A > 0$, the system is strictly hyperbolic. Note that

$$\frac{\partial \mathbf{F}}{\partial z} = \frac{\partial \mathbf{F}}{\partial \mathbf{U}} \frac{\partial \mathbf{U}}{\partial z} = \mathbf{H} \frac{\partial \mathbf{U}}{\partial z} \quad (8)$$

Let (ℓ_1, ℓ_2) and (r_1, r_2) be the left and right eigenvectors of matrix \mathbf{H} and let

$$\begin{aligned} \mathbf{L} &= [\ell_1, \ell_2]^T \\ \mathbf{R} &= [r_1, r_2] \\ \mathbf{\Lambda} &= \text{diag}(\lambda_1, \lambda_2) \end{aligned} \quad (9)$$

\mathbf{H} can be written as

$$\mathbf{H} = \mathbf{R} \mathbf{\Lambda} \mathbf{L} \quad (10)$$

Using the fact that the left and right eigenvectors are mutually orthogonal, i.e., $\mathbf{L} \mathbf{R} = \mathbf{I}$, equation 5 can be written as

$$\mathbf{L} \frac{\partial \mathbf{U}}{\partial t} + \mathbf{\Lambda} \mathbf{L} \frac{\partial \mathbf{U}}{\partial z} - \mathbf{L} \mathbf{B}(\mathbf{U}) = 0 \quad (11)$$

Assume that there exist functions W_1 and W_2 which satisfy

$$\frac{\partial W_i}{\partial \mathbf{U}} = \ell_i \quad \text{For } i = 1, 2 \quad (12)$$

We call $W_{1,2}$ characteristics of the hyperbolic PDE. For the case where the source term $\mathbf{B} = 0$ equation 11 can be decoupled as

$$\frac{\partial W_i}{\partial t} + \lambda_i \frac{\partial W_i}{\partial z} = 0 \quad (13)$$

from here we have W_1 and W_2 being constants along two characteristic curves

$$\begin{aligned} \frac{dz}{dt} &= \lambda_1 \\ \frac{dz}{dt} &= \lambda_2 \end{aligned} \quad (14)$$

Eigenvectors for \mathbf{H} is given by

$$\ell_{1,2} = \begin{bmatrix} \left(-\alpha\bar{u} \pm \sqrt{c^2 + \alpha(1-\alpha)\bar{u}^2} \right) / \left(c^2 - \alpha\bar{u}^2 \right) \\ 1 \end{bmatrix} \quad (15)$$

where \bar{u} is the average flow velocity and c is the wave propagation speed defined as

$$\bar{u} = \frac{Q}{A}, \quad c = \sqrt{\frac{\beta}{2\rho A_0}} A^{1/4} \quad (16)$$

Solving for W_1 and W_2 and the eigenvalues for \mathbf{H} we get

$$\begin{aligned} W_{1,2} &= \alpha\bar{u} \pm 4c \\ \lambda_{1,2} &= \alpha\bar{u} \pm \sqrt{c^2 + \alpha(1-\alpha)\bar{u}^2} \end{aligned} \quad (17)$$

We also note that the characteristics can be inverted to get Q and A using the following expressions

$$A = \frac{2\rho A_0^2}{\beta} \left(\frac{W_1 - W_2}{8} \right)^4, \quad Q = A \frac{W_1 + W_2}{2} \quad (18)$$

these expressions will be useful for boundary and compatibility condition considerations.

2.3 Numerical discretization

System (5) is discretized using Galerkin finite element method. Let V_h be the finite element space of piecewise linear functions and $V_h^0 = \{v_h \in V_h | v_h = 0 \text{ at } z = 0, L\}$ defined over the domain $z \in [0, L]$. We denote the L^2 scalar product as

$$\langle u, v \rangle = \int_0^L u \cdot v dz \quad (19)$$

the semi-discretized form of the system reads

$$\left\langle \frac{\partial \mathbf{U}}{\partial t}, \psi_h \right\rangle + \left\langle \frac{\partial \mathbf{F}}{\partial z}, \psi_h \right\rangle = \langle \mathbf{B}, \psi_h \rangle \quad \forall \psi_h \in V_h^0 \quad (20)$$

The time discretization is done using a Crank-Nicolson method. The final discretized system reads: find \mathbf{U}^{n+1} which satisfy

$$\left\langle \frac{\mathbf{U}^{n+1} - \mathbf{U}^n}{\Delta t}, \psi_h \right\rangle = \frac{1}{2} \left(\left\langle -\frac{\partial \mathbf{F}(\mathbf{U}^{n+1})}{\partial z} + \mathbf{B}(\mathbf{U}^{n+1}), \psi_h \right\rangle + \left\langle -\frac{\partial \mathbf{F}(\mathbf{U}^n)}{\partial z} + \mathbf{B}(\mathbf{U}^n), \psi_h \right\rangle \right) \quad (21)$$

where \mathbf{U}^n is \mathbf{U} at the current previous time step. This forms a set of nonlinear equations which is solved using Newton-Raphson iteration method.

2.4 Boundary conditions

In the physiological flow regime, the system requires exactly one boundary condition at each end of the domain. Furthermore, the system must be accompanied by compatibility conditions which reads

$$\begin{aligned}\ell_2^T \left(\frac{\partial \mathbf{U}}{\partial t} + \frac{\partial \mathbf{F}}{\partial z} - \mathbf{B} \right) &= 0, \quad z = 0 \\ \ell_1^T \left(\frac{\partial \mathbf{U}}{\partial t} + \frac{\partial \mathbf{F}}{\partial z} - \mathbf{B} \right) &= 0, \quad z = L\end{aligned}\tag{22}$$

To impose the compatibility conditions, a method called "characteristic extrapolation" is used to approximate the incoming and outgoing characteristic at the next time step. Characteristic extrapolation reads

$$W_2^{n+1}(0) = W_2^n(-\lambda_2^n(0)\Delta t), \quad W_1^{n+1}(L) = W_1^n(L - \lambda_1^n(L)\Delta t)\tag{23}$$

For the case of this implementation, a non-reflecting boundary condition is implemented. This boundary condition allow for the wave to not be reflected at the outlet end of the domain. Non-reflecting boundary condition requires that $W_2(L)$ is constant. With $W_2(L)$ constant, and $W_1(L)$ computed from the compatibility conditions above, we can use equations (18) to compute A and Q at the outlet boundary at time step $n + 1$.

2.5 Domain decomposition approach

Often times, one would like to access the wave propagation behavior of arteries in the presence of a prosthesis or a stent. These stents are grafted onto a section of the blood vessel as shown in figure 1. Computationally, the section with the stent has a significantly higher elastic modulus than that of the blood vessel. This discontinuity of the elastic modulus can cause numerical instability to the numerical method. One approach is to approximate the discontinuity with a continuous function as done in [5]. Essentially the discontinuity is smeared out over the transitional region. This method requires a very fine mesh at the the transitional region.

The approach utilized in this work is proposed in [2] which partitions the domain such that elastic modulus remains continuous as shown in figure 2. With this method, one will have to solve equation (21) for three separate domains. Each domains are coupled using their boundary conditions. Let us consider the process of coupling domain Ω_1 and Ω_2 from figure 2. Let Q_1^{n+1} and A_1^{n+1} be the flow rate and area at the outlet end of Ω_1 at time step $n + 1$. Furthermore let Q_2^{n+1} and A_2^{n+1} be the flow are and area at the inlet of Ω_2 at time step $n + 1$. The flow rate must be conserved and total pressure at the interface must be continuous, i.e.,

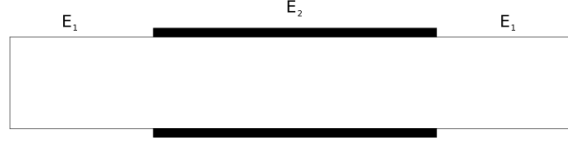


Figure 1: Schematic of blood vessel with arterial prosthesis. Blood vessel's elastic modulus is E_1 . The prosthesis's elastic modulus is E_2 .

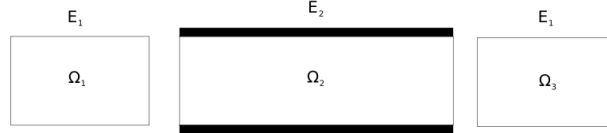


Figure 2: Schematic of the domain decomposition approach. Each domain now has a constant elastic modulus.

$$\begin{aligned} Q_1 &= Q_2 \\ P_1 + \frac{1}{2}\bar{u}_1^2 &= P_2 + \frac{1}{2}\bar{u}_2^2 \end{aligned} \quad (24)$$

where P_1, \bar{u}_1 and P_2, \bar{u}_2 are equations (4) and (16) evaluated at A_1^{n+1}, Q_1^{n+1} and A_2^{n+1}, Q_2^{n+1} respectively. These continuity relations are coupled with compatibility equations (23), where we use the W_1^{n+1} relation evaluated at the outlet of Ω_1 and W_2^{n+1} relation evaluated at the inlet of Ω_2 . We now have a set of 4 non-linear algebraic equations with 4 unknowns. These equations are solved using Newton-Raphson iteration method. Note here that the subscripts 1 and 2 in the characteristic equations refer to the \pm of the characteristics.

The continuity and compatibility equations are evaluated at the end of each time step to compute A_1^{n+1}, Q_1^{n+1} and A_2^{n+1}, Q_2^{n+1} which are then assigned as the boundary conditions for the next time step.

2.6 Bifurcation

To handle bifurcations, we employ a method similar to domain decomposition described above. As an example, let us consider a 'Y' shaped bifurcation shown in figure 3. Again, flow and area at the outlet of Ω_1 are denoted as Q_1 and A_1 . Flow and area at the inlet of Ω_2 and Ω_3 are denoted as Q_2, A_2 and Q_3, A_3 . The superscript $n + 1$ is omitted here for brevity. Continuity and mass conservation demands that

$$\begin{aligned} Q_1 &= Q_2 + Q_3 \\ P_1 + \frac{1}{2}\bar{u}_1^2 &= P_2 + \frac{1}{2}\bar{u}_2^2 \\ P_1 + \frac{1}{2}\bar{u}_1^2 &= P_3 + \frac{1}{2}\bar{u}_3^2 \end{aligned} \quad (25)$$

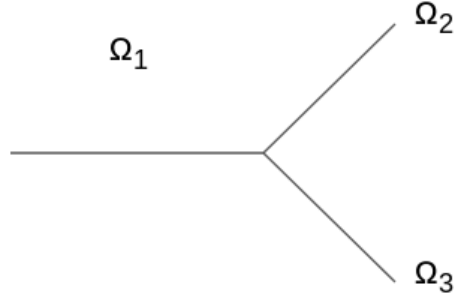


Figure 3: Example 'Y' shaped bifurcation

These equations are coupled with compatibility equations, one for each vessel to form a set of 6 non linear equations and 6 unknowns to be solved numerically.

Using the relations described above, one can devise the set of nonlinear equations describing a bifurcation with with 1 parent vessel and n daughter vessels as follows. Let subscript p denote quantities at the outlet of the parent vessel and subscript di denote quantities at the inlet of daughter vessel i , the set of $2n + 2$ equations read

$$\begin{aligned}
 Q_p - \sum_{i=1}^n Q_{di} &= 0 \\
 P_p + \frac{1}{2}\bar{u}_p^2 &= P_{di} + \frac{1}{2}\bar{u}_{di}^2 \quad \forall i \in [1, n] \\
 W_{1,p}^{n+1}(L) &= W_{1,p}^n(L_p - \lambda_1^n(L_p)\Delta t) \\
 W_{2,di}^{n+1}(0) &= W_{2,di}^n(-\lambda_{2,di}^n(0)\Delta t) \quad \forall i \in [1, n]
 \end{aligned} \tag{26}$$

These equations are solved at the end of each time step for the boundary conditions at the next time step. These conditions along with an appropriate inlet boundary condition at the parent vessel completes the solution procedure.

3 Results

In this section, a test case of the model is presented. In the test cases, blood is assumed to have density $\rho = 1g/cm^3$, viscosity $\nu = 0.035poise$. The vessel wall has elasticity $E = 3 \times 10^6 dyne/cm^2$, wall thickness $h_0 = 0.05cm$, and initial radius is $r_0 = 0.5cm$. A single pulse sine wave is applied at the inlet of the parent vessel with amplitude of $P_0 = 20 \times 10^3 dyne/cm^2$.

Three test problems are considered in this case study. First, a model based on figure 1 where $E_1 = E_2 = E_3$ is considered. This case represents a healthy vessel without a prosthesis. A second case considered is when $E_2 = 100E_1$. This is a case where an arterial prosthesis is applied. Domain Ω_2 starts at $z = 5cm$ and ends at $z = 10cm$. A third case is based on the model outlined in figure 3. The bifurcation point occurs at $z = 5cm$ which is the same point as where the prosthesis is applied of the second test case. Each vessel has the same wall properties. The following figures plot pressure over time as sampled in the center of each domain.

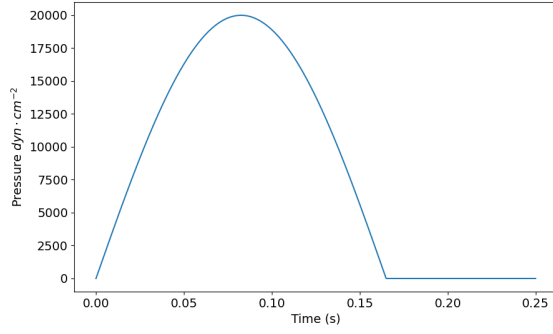


Figure 4: Input pressure

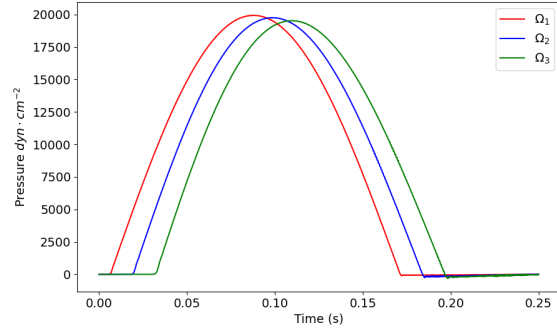


Figure 5: Pressure wave without prosthesis.

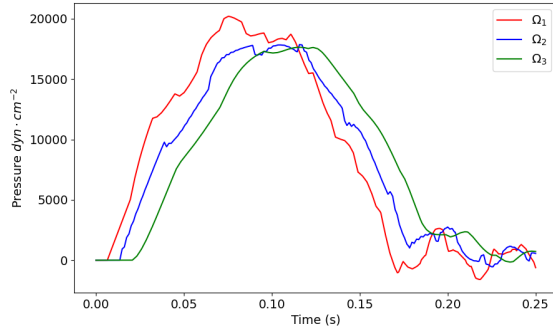


Figure 6: Pressure wave with prosthesis.

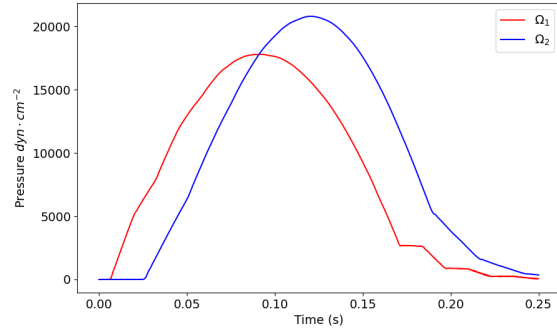


Figure 7: Pressure wave for bifurcating vessel.

4 Discussion

The baseline case shown in figure 5 show no wave reflection along each domain. A slight damping is observed, this is due to the viscosity of the flow. For the case where a prosthesis is applied, we observe high frequency contents particularly in Ω_1 . This is because the prosthesis is much stiffer than healthy artery causing reflection at a high frequency content. For the case of a bifurcating vessel, we observe wave reflections occurring in Ω_1 as well. Since the vessel properties remain the same, we do not see high frequency contents in the bifurcating vessels case.

5 Conclusion

In this work, an implementation of the 1 dimensional arterial flow model is presented. Domain decomposition is used to account for bifurcations and discontinuity of parameters in the system. The model is solved using Galerkin finite element method. An example case of wave reflection due to arterial prosthesis and bifurcation is presented.

References

- [1] Martin S. Alnæs, Jan Blechta, Johan Hake, August Johansson, Benjamin Kehlet, Anders Logg, Chris Richardson, Johannes Ring, Marie E. Rognes, and Garth N. Wells. The fenics project version 1.5. *Archive of Numerical Software*, 3(100), 2015.
- [2] Luca Formaggia, Daniele Lamponi, and Alfio Quarteroni. One-dimensional models for blood flow in arteries. *Journal of Engineering Mathematics*, 47(3/4):251–276, December 2003.
- [3] Alfio Quarteroni and Luca Formaggia. Mathematical modelling and numerical simulation of the cardiovascular system. In *Handbook of Numerical Analysis*, pages 3–127. Elsevier, 2004.
- [4] Irene E. Vignon-Clementel, C. Alberto Figueroa, Kenneth E. Jansen, and Charles A. Taylor. Outflow boundary conditions for three-dimensional finite element modeling of blood flow and pressure in arteries. *Computer Methods in Applied Mechanics and Engineering*, 195(29-32):3776–3796, June 2006.
- [5] Jing Wan, Brooke Steele, Sean A. Spicer, Sven Strohband, Gonzalo R. Feijo´o, Thomas J.R. Hughes, and Charles A. Taylor. A one-dimensional finite element method for simulation-based medical planning for cardiovascular disease. *Computer Methods in Biomechanics and Biomedical Engineering*, 5(3):195–206, January 2002.